Research on Chemical Intermediates (2021) 47:3363–3378
https://doi.org/10.1007/s11164-021-04461-3

Ultrasound/visible light-mediated synthesis of N-heterocycles using g-C_3N_4/Cu_3TiO_4 as sonophotocatalyst

Murugan Arunachalapandi[1] · **Selvaraj Mohana Roopan**[1]

Received: 18 January 2021 / Accepted: 29 March 2021 / Published online: 9 April 2021

Abstract

In this investigation, novel g-C_3N_4/Cu_3TiO_4 (CNCT) nanocomposite was synthesized by using a simple thermal condensation method. The synthesized CNCT nanocomposite was characterized by X-ray Diffraction, Transmission electron microscopy, Atomic force microscopy, Energy-dispersive X-ray spectroscopy, X-ray photoelectron spectroscopy, UV–vis diffuse reflectance spectroscopy, Photoluminescence, Brunauer–Emmett–Telle, Zeta Potential, and Thermogravimetric analysis. The study revealed that the catalysts prepared have high crystalline nature, optical light-absorbing property, high surface area, and stability. The CNCT- nanocomposite was found to be an extraordinary visible light absorbing catalyst for the synthesis of quinoxaline and quinazolinone derivatives, which have important benefits in a variety of drug applications. Quinoxaline and quinazolinones were prepared from anthranilamide, diamines, benzil, and corresponding aldehydes under Ultrasonic/visible light-medium with a notable amount of g-C_3N_4/Cu_3TiO_4. The results exhibit good and excellent yields of product derivatives at mild conditions under Ultrasonic/visible light-medium. Ultrasounds always clean the active site catalyst, promoting activity and reusability. Most notably, with preserved reactivities, this heterogeneous g-C_3N_4/Cu_3TiO_4 composite can be used atleast 5 times. Furthermore, we examined the reusability of the catalyst under Ultrasonication coupled with Visible light and in the absence of an Ultrasonication medium. Finally, advantages of the method are non-conventional approach, green solvent, reduced reaction duration, mild condition, and reusable catalyst.

Keywords G-C_3N_4 · Cu_3TiO_4 · Visible light · Quinoxaline · Quinazolinone

✉ Selvaraj Mohana Roopan
mohanaroopan.s@vit.ac.in

[1] Chemistry of Heterocycles and Natural Product Research Laboratory, Department of Chemistry, School of Advanced Sciences, Vellore Institute of Technology, Vellore, Tamil Nadu 632 014, India

Introdction

Heterocycles are mostly used in the field of medicinal chemistry. Heterocycles motifs of quinazolinones and quinoxalines are present in drugs such as luotonine, Rutaecarpin, Tryptanthrin, Chloroqualone, and alloqualone [1, 2]. The core structure of quinazolin-4(3*H*)-ones and quinoxaline makes them interconvertible in heterocycles family. Quinoxalines have enormous applications in antibacterial, antidiabetic, antimalarial, and antifungal properties [3–5]. Hence quinoxaline and quinazolinone were used as a template for the development of many drugs [6]. Biological applications of quinazolinone show remarkable properties such as high molar extinction coefficient, absorption, fluorescence emission, and fluorescence quantum yield [7]. An additional property of quinazolinones was an optical character in light-emitting diodes, cell imaging, and sensors [8]. Already plenty of preparation techniques were published for the synthesis of quinoxaline and quinazolinones. We have the challenge to produce a new method to prepare these compounds which is an easy and better method to compare with others. Here we introduce a new nonconventional approach for the preparation of quinazolinone with the use of ultrasonication/visible light with a 20% CNCT catalyst.

In this decade, nanoparticles gained more attention to scientists to do more attractive innovations (Sensors, semiconductors, nanobots, photocatalysts, etc.). Homogeneous and Heterogeneous catalysts are mostly used in organic reactions to enhance the reaction [9]. Some of the drawbacks present in homogeneous catalysts such as reusability, removal from the reaction mixture, and stability in the reaction medium are difficult. On the other hand, heterogeneous catalysts can easily overcome all these problems and produce excellent lower activation energy for the reaction. Here, heterogeneous catalyst was used to carry out the condensation reaction in presence of light and sound [10].

Graphitic carbon nitride (g-C_3N_4) a polymer material is rich in carbon and nitrogen atoms. Recently, g-C_3N_4 has gained more attention and it is mostly used to bind with metal nanoparticles which are used for the photocatalytic degradation of pollutants, CO production, biosensors, semiconductors, etc. [11]. In organic synthesis, the g-C_3N_4 assisted CNCT material showed great promise in photocatalysis, with excellent visible light properties (eV = 2.7), high stability, efficient reusability, ease of removal from the reaction mixture, and good semiconductor properties [12]. In the past five decades, photocatalytic titanium dioxide was invented by Honda and Fujishima for splitting water [13]. After that TiO_2 has applied for many organic reactions such as degradation of organic dyes, cycloadditions, oxidation, reduction, and cross-coupling reactions [14]. Titania (TiO_2) is a UV light active material (3.1 eV) that is easily available and costless material. Normally, CuO and TiO_2 are not much active in the visible region. By coating the semiconducting material Cu_3TiO_4, on the polymeric surface of g-C_3N_4 made it active in visible light. In this study, heterocycles were synthesized in the presence of CNCT using ultrasonication and visible light.

Materials and methods

Chemicals utilized

The Citrus Lemons were collected from Vellore local market shop, Vellore, Tamil Nadu, India. All chemicals were purchased from AVRA, chemical Pvt. Ltd, and Hyderabad. Throughout the experiment process, we utilized double distilled water without any further purification.^{1}H NMR and ^{13}C NMR spectra were taken by using 500 MHz Bruker DRX-500 and TMS as an internal standard.

Preparation of extract

The lemon extract was prepared using the conventional method [15]. 50 mL of liquid lemon juice was centrifuged at 10,000 rpm. The aqueous solution was collected and stored for future usage. The pulp and other impurities were separated.

Synthesis of g-C_3N_4

g-C_3N_4 was prepared by a simple condensation method [16]. The parent compound melamine monomer was used to prepare g-C_3N_4 polymer. About 5 g of melamine powder was heated at 550 °C for 4 h. The formation of the polymer was confirmed by a change of color white to yellow. The collected yellow precipitate was crushed in mortar pestle and made into fine crystals.

Synthesis of Cu_3TiO_4

1 M copper acetate was dissolved in 50 mL of deionized water and added 1 M of titanium butoxide dropwise into the solution with constant stirring. The solution was stirred with 5 mL of lemon extract for 2 h. Here bluish-white color precipitate was obtained after 1 h. Then the precipitate was kept in a water bath. The precipitate was washed with deionized water followed by ethanol and then calcinated for 4 h at 500 °C.

Synthesis of CNCT

About 0.1 g of prepared Cu_3TiO_4 and 0.9 g of g-C_3N_4 were mixed in different ratios (Table. S1), with 5 mL of water and this mixture was kept in stirring for 2 h. The obtained suspension was sonicated for 20 min via ultrasonication. Then, the solution was kept for drying on a hot-air oven 50 °C. Finally, obtained light blackish yellow precipitate was calcinated at 300 °C for 2 h.

General procedure for the synthesis of quinoxalines (1.3a–1.3l)

Method A

Benzil **1.1** (1 mmol), *O*-phenylinediame **1.1** and (2 mmol) 40 mol% of 20% CNCT in ethanol (5 mL) was taken in a boiling tube. The reactants were stirred at 45 °C in an oil bath. Thin Layer Chromatography (TLC) is a tool to find out the reaction completion. After completion of the reaction from TLC hot ethanol was added to the reaction mixture. The solution was filtered which leads to separate the catalyst. Then the remaining filtrate was poured into cool water to get solid. The precipitate was separated and recrystallized from hot ethanol to obtain the final compound.

Method B

As per method A, the same quantity of the reactants were taken and placed in an ultrasound/visible light for 10 min (Table 1, entry 10). Reaction workup and purification were done as per method A.

General procedure for the synthesis of dihydro quinazolinone (2.3a–2.3h)

For the preparation of quinazolinone, a similar procedure optimized for the quinoxaline **2.3** was followed. The reactants used for this preparation were anthranilamide **2.1** (1 mmol), benzaldehyde **2.2** (1 mmol), 20% CNCT (40 mol%), solvent (5 mL) for 10 min.

Characterization

X-ray diffraction (XRD) patterns were obtained from The Bruker, D8 advance PC system with Cu Kα ($\lambda = 1.544$) as X-ray source. The range to carry out the output was 10°–90° (2θ). The morphology of the prepared samples were characterized by Transmission electron microscope (TEM) Tecnai G2-20 instrument. Bruker EDX with LN2 free detector was employed to conduct EDAX analyses. On using Quanta chrome analyser, the surface area assessment of the acquired nanocomposite was established at 77.35 K by N_2 adsorption/desorption isotherm. Samples of 0.1262 g analyzed fix final gas temperature at 200 °C. The BET surface area was calculated by a multi-point BET isotherm, whereas the BJH method was used to measure the

Table 1 Stability comparison of prepared nanocomposite

Entry	Compound	Zeta value (mV)	Nature
1	g-C_3N_4	− 33.6	Good stable
2	Cu_3TiO_4	− 33.9	Good stable
3	20% CNCT	− 34.7	Good stable

pore size distribution. Zeta potential (HORIBA SZ-100) was used to record the stability and surface charge of the constructed nanocomposite. PHI 5000 Versa Probe III instrument was employed to record X-ray photoelectron spectroscopy (XPS) with reference to the C 1*s* peak (282.8 eV). The thermogravimetric and differential scanning calorimetry (TG-DSC) were analysed at 20 °C min^{-1} to 800 °C in the air by using an SDT Q600 analyzer. Jasco V-670 spectrometer was employed to record the diffuse reflectance absorption spectra (DRS). FLSP920 (Edinburgh, UK) spectroscope was used to record the photoluminescence (PL) spectra. The F-7000 FL spectrophotometer with an equipped excitation wavelength of 280 nm was used to collect the photo-luminescence spectrum.The excitation wavelength was 447 nm.

Results and discussion

Among all the catalysts, 20% CNCT showed better yield than others (Cu_3TiO_4, 5% CNCT, 10% CNCT, 30% CNCT). Therefore, 20% CNCT was used for further characterisation. The phase purity and crystalline nature of synthesized CNCT nanocomposite were analysed using X-Ray Diffraction (XRD) analysis. XRD pattern for the prepared g-C_3N_4, Cu_3TiO_4 and CNCT nanocomposites is shown in Fig. 1a. XRD pattern of Cu_3TiO_4 was indexed as (004) (101) (102) (106) and (110) found at $\theta = 86.4$, 54, 69.1, and 32.5 ° for Cu_3TiO_4 nanocomposite (JCPDS Card no. 83–1285). Cu_3TiO_4 nanospheres were used for the further binding with g-C_3N_4 like 5%, 10%, 20%, and 30% (Fig. 1b). In 5% CNCT XRD shows the same mirror image of g-C_3N_4. Slightly Cu_3TiO_4 peaks appears in 10% CNCT and then increase the intensity in 20% & 30% CNCT. The crystalline size and strain were calculated using Scherer formula, which is 47.4 nm. Two peaks absorbed at the region of 13.2°, 27.4° were indexed as (110) and (002) for g-C_3N_4 (JCPDS, 87-1526). The XRD of the combined 20% CNCT nanocomposite perfectly match with its individual XRD of g-C_3N_4, TiO_2, CuO, and Cu_3TiO_4 (Fig. 1).

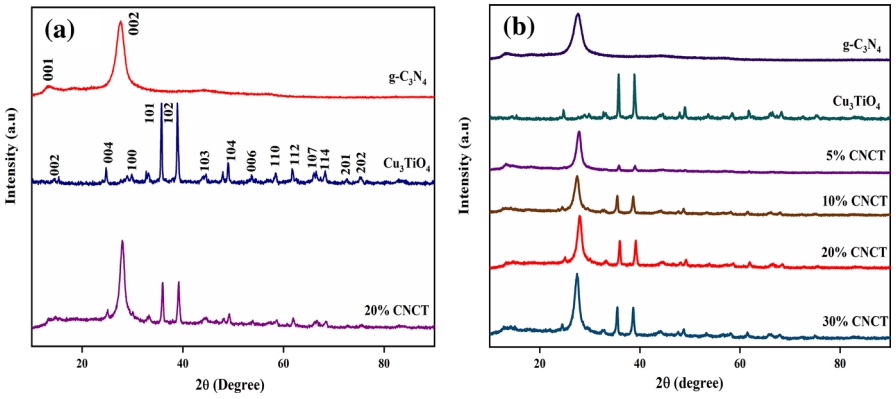

Fig. 1 **a** XRD of Cu_3TiO_4, g-C_3N_4, and 20% CNCT **b** XRD of CNCT composites synthesized at different concentrations

To check the stability nature of 20% CNCT nanocomposite zeta potential analysis was used. In the present study, 20% of CNCT nanocomposites were having a good surface charge as shown in Table 1. The zeta potential value for 20% CNCT and Cu_3TiO_4 nanospheres was − 34.7 mV and − 33.9 mV (Table 1, Entry 2, 3) which indicated that the prepared nanocomposite possesses high stability.

Transmittance Electron Microscope (TEM) study has shown the surface morphology of 20% CNCT (Fig. 2). Here, TEM images of 1% Cu_3TiO_4 nanospheres are given in Fig. 2a. This image showed sphere-like morphology of Cu_3TiO_4. After binding, the spheres of Cu_3TiO_4 were deposited on the sheets of g-C_3N_4, (Fig. 2c). Particle size for Cu_3TiO_4 was observed at around 47 nm from XRD results which was confirmed in TEM images. Figure 2b shows the clear sheets of g-C_3N_4 without support. After binding Fig. 2c indicates the layered g-C_3N_4 was decorated by nanospheres of Cu_3TiO_4. Sheets were decorated with Cu_3TiO_4 nanospheres that are clearly shown in Fig. 2c. The selected area electron diffraction (SAED) is shown in Fig. 2d. SAED belongs to the plane (111) of hexagonal Cu_3TiO_4 in the nanocomposite, the high crystalline structure of the sample was shown by bright spots. The SAED results were very consistent with the XRD results. Determination of the elements present in 20% CNCT nanocomposite was done by Energy dispersive X-ray (EDX). EDX spectrum of 20% CNCT nanocomposite is shown in Fig. 2f. EDX spectrum indicates that the presence of target alone in the material. Moreover, it was proved that the compound is pure and no other elements were formed. 20% CNCT has copper, titanium, oxygen, carbon, and nitrogen (Table 2). To explain the topological appearance of 20% CNCT nanocomposite, AFM analysis is shown in Fig. 2e. CNCT nanocomposites revealed that Cu_3TiO_4 crystals were partly sprayed on g-C_3N_4 surface. Crown and smooth-like pictures of g-C_3N_4 and CNCT are depicted in Fig. 2e. For photocatalytic reaction, the specific surface area of catalyst can be detected from the above nitrogen adsorption–desorption isotherm values (Table 3) of g-C_3N_4 and 20% CNCT sample.The minor improvement after the assistance of Cu_3TiO_4 on the g-C_3N_4 surface is shown in both values (Table 3, Entry 1, 3). There is a small increase in CNCT surface area and pore volume, which means an increase in catalyst reactant adsorption potential relative to g-C_3N_4.

To test the oxidation state of elements by X-ray photoelectron spectra (XPS) were used. A survey graph of 20% CNCT nanocomposite is shown in Fig. 3a, it represents the major elements of C1*s*, N1*s*, Cu2*p*, Ti2*p*, and O1*s*. As stated in Fig. 3b, the asymmetrical and large characteristics of C1*s* XPS peaks observed indicates that distinguishable versions co-exist. Sp^2-hybridized carbons (C–C) produced a sharp peak at the range of 284.6 eV [17]. 398.8 eV-centered peak is for sp^2 N involved in triazine rings (Fig. 3c), while 399.6 eV peak corresponded to C bridged nitrogen atoms. Cu(I) bonded with oxygen atoms is executing a sharp peak at 133,1 eV.Cu(II) peaks presence (Fig. 3d) was confirmed at 941.8 eV, 953.3 eV, 964.7 eV. Here the confirmation of Cu(I) and Cu(II) atoms were present in 20% of CNCT. As seen from Fig. 3e, we find that XPS peaks of Ti2*p* exhibit two signal peaks at 458.2 that were attributed towards the Ti^{4+} species. Figure 3f attributed to O1*s* corresponds to two sharp peaks at 529.6 and 531.4 eV, which shows the presence of O atoms.

Ultraviolet (UV) visible spectroscopy is a tool to identify the absorption region of synthesized nanocomposites. In the present study, 20% CNCT, g-C_3N_4, Cu_3TiO_4

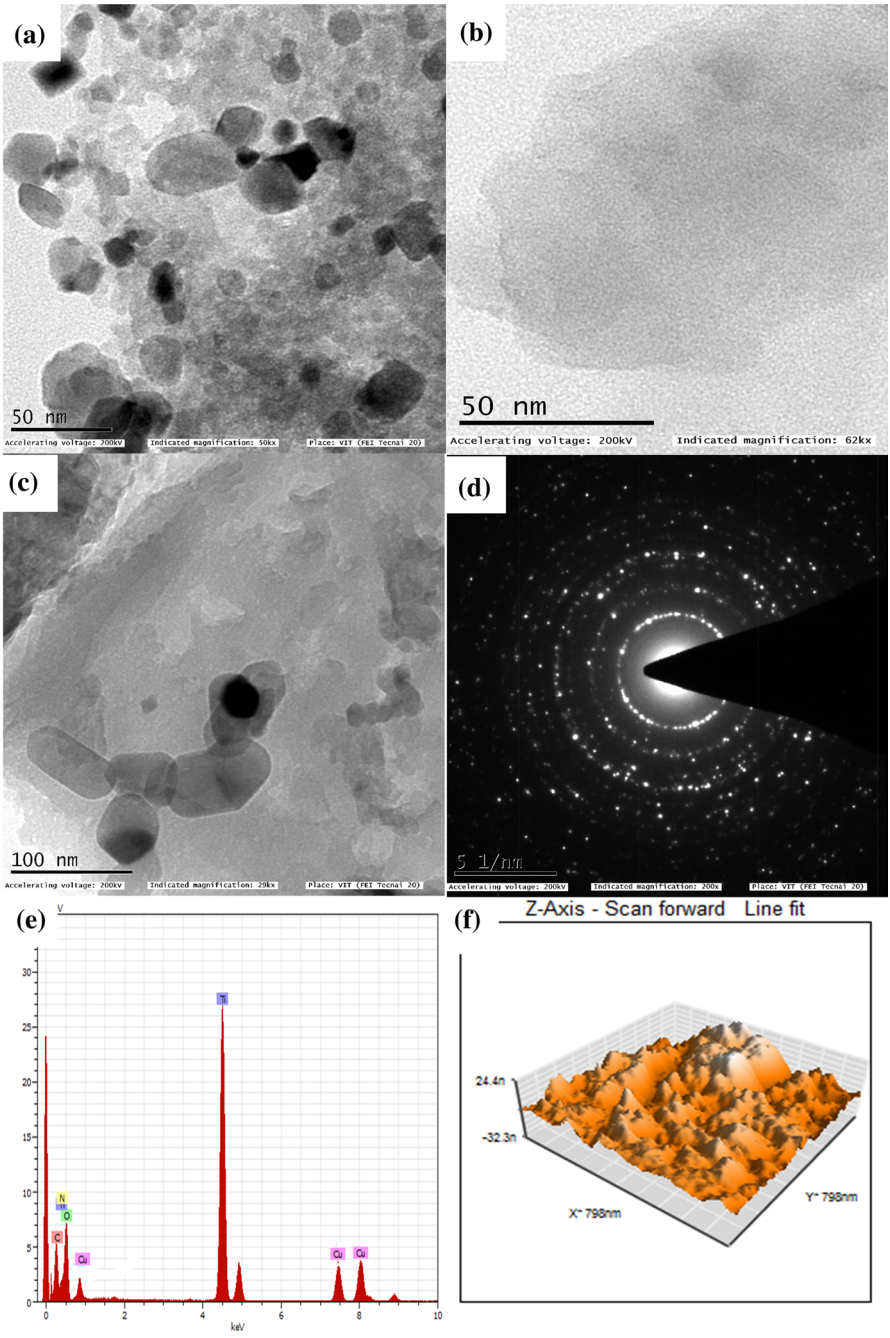

Fig. 2 TEM images of **a** 1% Cu_3TiO_4 nanospheres, **b** g-C_3N_4, **c** 20% CNCT, **d** SAED patterns of 20% CNCT, **e** EDX spectrum of 20% CNCT, **f** AFM analysis of 20% CNCT nanocomposites

Table 2 The amount of elements in 20% CNCT

Entry	Element	Serious	wt%
1	Carbon	K-serious	43.01
2	Nitrogen	K-serious	15.22
3	Copper	K-serious	1.45
4	Titanium	K-serious	23.71
5	Oxygen	K-serious	16.61

Table 3 Surface studies of 20% CNCT nanocomposite wit BET analysis

Entry	Compound	Surface area	Pore volume (cc/g)	Pore diameter (Å)
1	g-C_3N_4	14.209	0.075	18.991
2	Cu_3TiO_4	2.739	0.016	6.922
3	20% CNCT	15.238	0.085	18.968

were analyzed using the UV-DRS spectrum as shown in Fig. 4a. The UV spectrum shows no absorption peak maximum for Cu_3TiO_4. After binding with g-C_3N_4, it has a strong peak at 384 nm. From Tauc's plot (Fig. 4b) we can calculate the energy gap (bandgap) value 2.68 eV corresponding to 20% CNCT. This shows the 20% CNCT have high activity in the visible region.

An indicator of electron–hole recombination rate for 20% CNCT nanocomposite with photoluminescence (PL) spectrum. 20% CNCT shows widespread emission peak at 430–470 nm, transition indicates the oxygen vacancies in the nanocomposite. Here absorbance intensities are directly related to the recombination rate of the catalyst. Figure 5 spectra show 20% CNCT has less intense peaks when compared to the g-C_3N_4 and Cu_3TiO_4 peaks. That is evidence for the suppression of electron–hole pair recombination and charge carriers separation in 20% CNCT [17–19].

Thermogravimetric analysis (TGA) is an analytical tool used to assess the thermal stability of a substance. TGA analysis of the prepared nanocomposite is shown in Fig. 6. 20% CNCT and g-C_3N_4 are having a lower diffusion temperature than Cu_3TiO_4 nanospheres. Figure 6 shows a strong evidence that our catalyst doesn't have any impurities (hydrocarbon, water, hydroxyls, etc.). Because 20% CNCT, g-C_3N_4, and Cu_3TiO_4 are don't have any diffusion point upto 600 °C. In Fig. 6 a straight line indicates no diffusion point for the Cu_3TiO_4 nanospheres. For g-C_3N_4, after 600 °C has strong diffusion and produce 0.6 wt% residue of carbon. In the case of 20% CNCT the same diffusion begins after 600 °C but 20 wt% residue remains. It informs the formation of CNCT.

Benzil **1.1** and diamines **1.2**, as a model reaction (Scheme 1) we have done 18 trials conducted to determine the conditions for the reaction. We attempted to refine the model process (method A) to describe the efficiency of several classic conditions for comparison. In each case of ultrasonic irradiation (40 kHz) conditions, ethanol was used as a solvent and tipping the ultrasonic rod was dipped into the reaction mixture. The formation of product **1.3** was easier among the solvents tested

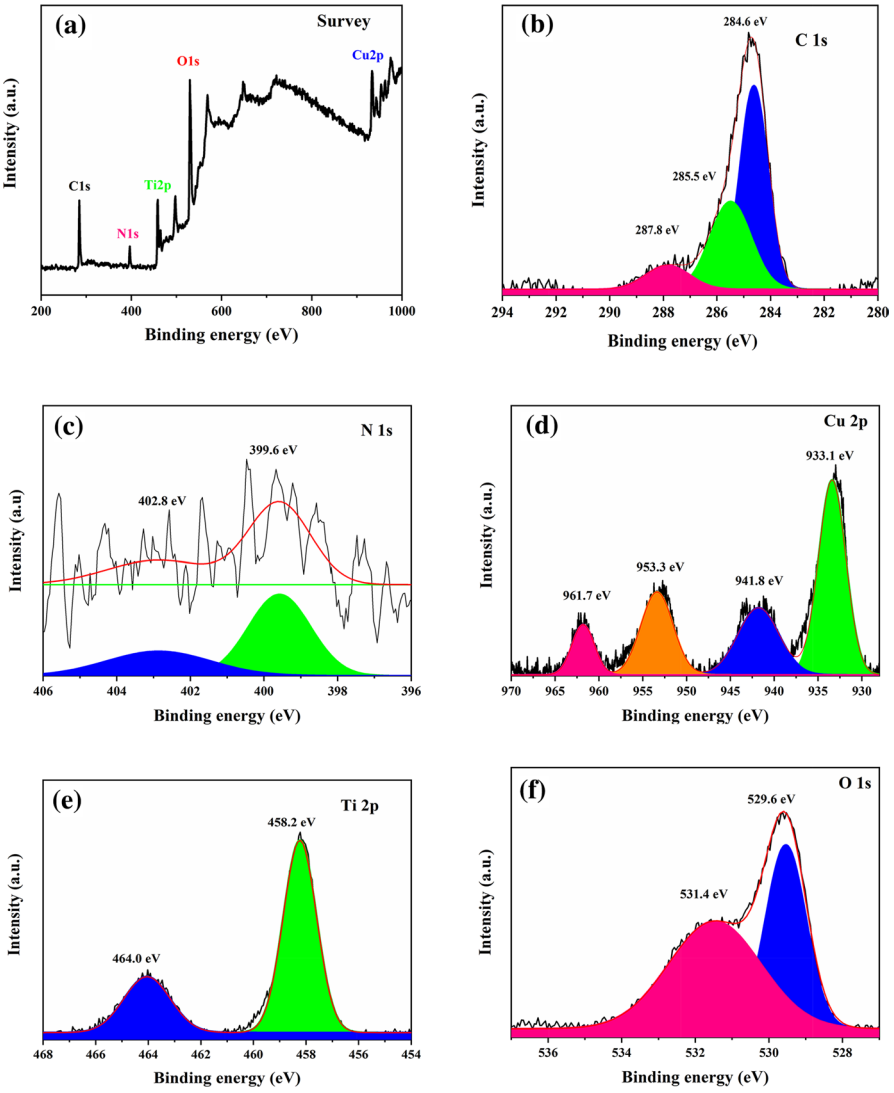

Fig. 3 XPS survey spectrum of **a** prepared 20% CNCT and the corresponding high-resolution XPS spectra of **b** C1*s*, **c** N1*s*, **d** Cu 2*p*, **e** Ti 2*p*, **f** O 1*s*

such as ethanol, H_2O, tetrahydrofuran (THF), dichloromethane (DCM), and solvent-free condition. Scheme 1 also produces a moderate yield in water (Table 4, Entry 11). But ethanol produced more yield than water. Therefore, ethanol was taken as a primary solvent for Schemes 1 and 2. Scheme 1 was performed in acetonitrile, THF, and DCM the target product was separated at 50%, 50%, and 63%, respectively (Table 4, Entries 12, 13, 14). The products **1.3** and **2.3** were not obtained without the catalyst conditions (Table 4, Entry 15). To check the efficiency of ultrasound/visible light irradiation, Scheme 1 was also carried out by the conventional method of

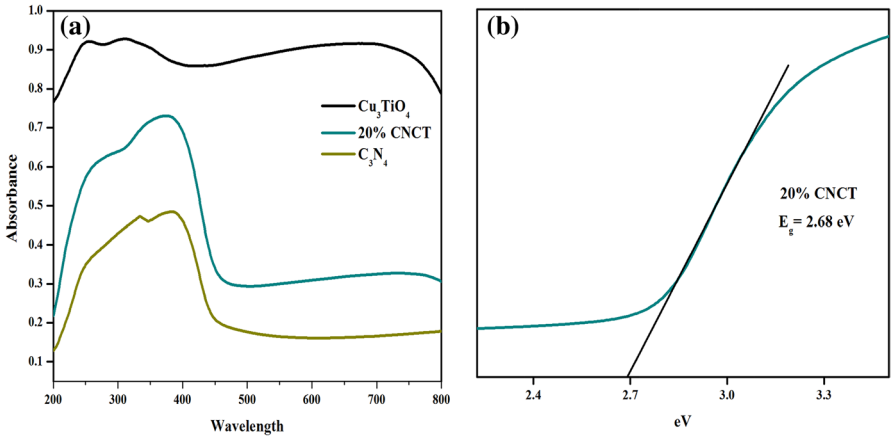

Fig. 4 **a** UV visible spectrum of Cu_3TiO_4, g-C_3N_4, and 20% CNCT, **b** bandgap image of 20% CNCT nanocomposite

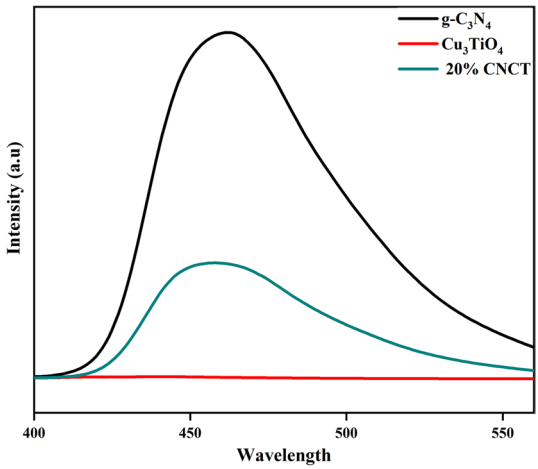

Fig. 5 Photoluminescence spectrum of 20% CNCT at different concentration

heating at 45 °C in with ethanol (Table 4, Entries 1, 2, 3, 4). Ultrasound and visible light conditions give more yields at a minimum time of 3–5 min (Table 4, Entry 10).

A comparatively minimum yield is absorbed in light-free reaction conditions, as shown in Table 4, Entry 7. We found that the presence of visible light, as shown in Table 4—Entry, 6, 8, and 11 could increase the reaction production and shorten the reaction time. The above studies revealed that this reaction had a remarkable ultrasonic temperature effect. Scheme 1 was also carried out at 30, 40, and 50 kHz to validate the effect of frequency in the reaction. With an increase in the level of irradiation from 40 to 50 kHz, the reaction yield did not change substantially (98% in a similar time, Table 4, Entry 10). The performance of CNCT was carried out under ultrasound/visible light irradiation. For

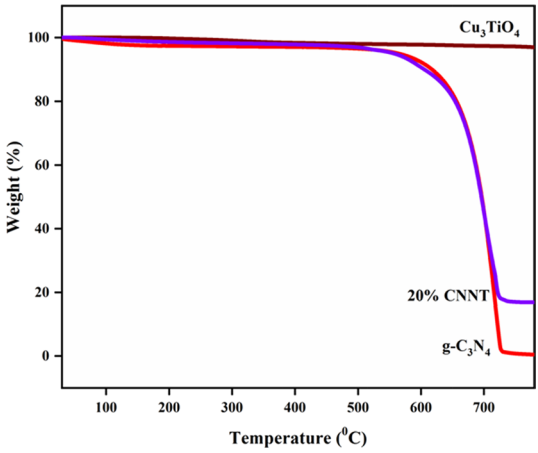

Fig. 6 Termogravimetric analysis of 20% CNCT

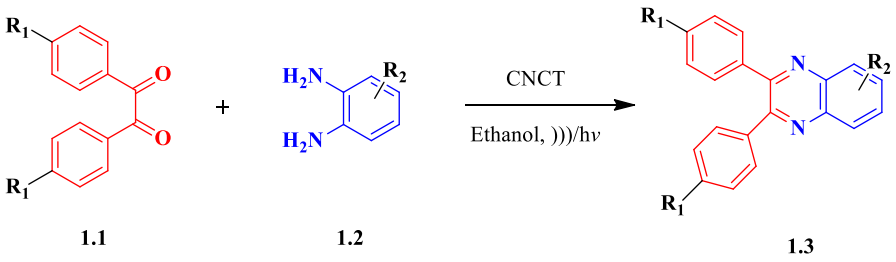

Scheme 1 Synthesis of quinoxalines

5% CNCT produced 56% of **1.3**. 10% CNCT has increased the yield of **1.3** upto 76%. Further, 20% CNCT with ultrasound/visible light irradiation shown a 98% yield. Photoluminencence spectra of 20% CNCT have an excellent electron–hole recombination rate. Then 30% CNCT also produced the same activity like 20% CNCT to yield 98% of the product. 20% CNCT was investigated in Schemes 1 and 2 for many substituted aryl or heteroaryl aldehydes, benzil, and diamines with ethanol (Table 4, Entry 15). When the reaction was conducted using conventional methods, the product was good but the reaction time was longer. Therefore, it was observed that ultrasonic irradiation had a beneficial impact on the synthesis of quinoxaline derivatives. Once we got the best reaction condition to carry out Scheme 1 with 98% of yields with 11 derivatives (Table 5). In Fig. 7 the reaction begins on the surface of g-C_3N_4. 1.1 has two active O2 sites where the reaction is initiated. **1.2** which has a lone pair of electron in N-atom reacts with the active sites to form a hydroxyl radical, releasing a water molecule and finally forming the final product **1.3**. The same condition was used to carry out Scheme 2 for the preparation of di-hydroquinazolinones in visible light/ultrasonication. This reaction was taken by carrying out in the absence of (Light/sound) at 70 °C for 45 min where 77% of yields were obtained. Then we proceed to carry

Table 4 Optimization for the synthesis of quinoxalines under ultrasonic and visible light irradiation

Entry	Catalyst	Solvent	Reaction condition	Time	Yield
1	CuO	ETOH	Δ	8 h	63
2	TiO_2	ETOH	Δ	8 h	32.5
3	$Cu(OAc)_2$	ETOH	Δ	8 h	27.5
4	$Zn(OAc)_2$	ETOH	Δ	8 h	26
5	g-C_3N_4	ETOH	Visible light	90 min	No reaction
6	Cu_3TiO_4	ETOH	Visible light	90 min	72
7	20% CNCT	ETOH	Δ	8 h	80
8	20% CNCT	ETOH	Visible light	90 min	92
9	20% CNCT	ETOH	Ultrasonication	30 min	88
10	20% CNCT	ETOH	Ultrasonication/visible light	10 min	98
11	20% CNCT	H_2O	Visible light	90 min	79
12	20% CNCT	DCM	Δ	8 h	63
13	20% CNCT	Acetonitrile	Δ	8 h	50
14	20% CNCT	THF	Δ	8 h	50
15	Without	ETOH	Δ	8 h	No reaction
16	5% CNCT	ETOH	Ultrasonication/visible light	10 min	56
17	10% CNCT	ETOH	Ultrasonication/visible light	10 min	76
18	30% CNCT	ETOH	Ultrasonication/visible light	10 min	98

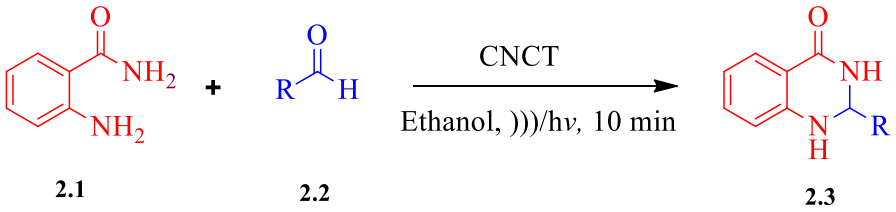

Scheme 2 Synthesis of quinazolinones

out in the presence of visible light where within ~ 10 min products were obtained with 97% of yields. Sonication was introduced to increase the efficiency of catalysts in recyclability. Without sonication, the first reaction gave excellent yields in 10 min. But a slight decrease in efficiency of the catalyst was seen in the next runs. This happened when the reactants attacked g-C_3N_4 active sites to reduce the activity. But in presence of sonication, g-C_3N_4 surface was refreshed to reduce the reactants blocking the active sites. Sonication plays a vital role in this reaction to increase the reusability of CNCT. The reaction occurred on the surface of 20% CNCT nanocomposites in ~ 5 min. Eight different derivatives including electron-donating, electron-withdrawing, and halogen compound were prepared in visible light and the ultrasonication method is shown in Table 6.

Because of its excellent photocatalytic behavior, nanocomposites supported with g-C_3N_4 were used as photocatalysts for the synthesis of quinazolinone and

Table 5 CNCT catalysed synthesis of Quinoxalines under ultrasonic and visible light irradiation[a]

Product	R_1	R_2	Time (min)	Yield[b]		Melting point		TON[d]	TOF[d]
				US/vis[c]	Δ[c]	Found	Ref.		
1.3a	H	H	5	98	23	125–126	[20]	6.2	1.24
1.3b	H	CH_3	5	92	21	120–122	[20]	5.8	1.16
1.3c	H	Cl	5	89	13	121–122	[20]	5.6	1.13
1.3d	H	NO_2	3	95	43	139–142	[20]	6.0	2.01
1.3e	CH_3	H	5	91	32	146–147	[20]	5.11	1.02
1.3f	CH_3	CH_3	5	89	29	129–130	[20]	5.00	1.00
1.3g	CH_3	Cl	5	88	12	115–117	[20]	4.95	0.99
1.3h	CH_3	NO_2	3	93	38	121–123	[20]	4.29	1.433
1.3i	Br	H	5	92	17	131–134	[20]	3.35	0.67
1.3j	Br	Cl	5	93	15	117–119	[20]	3.38	0.67
1.3k	Br	NO_2	3	83	33	112–113	[20]	3.02	1.00

[a]Reaction condition: benzil (1 mmol), diamine (2 mmol), catalyst (40 mg) were simultaneously treated with ultrasonic and visible light irradiation

[b]Isolated yields

[c]*US* ultrasonic, *VS* visible light, Δ conventional heat

[d]*TON* turn over number, *TOF* turn over frequency

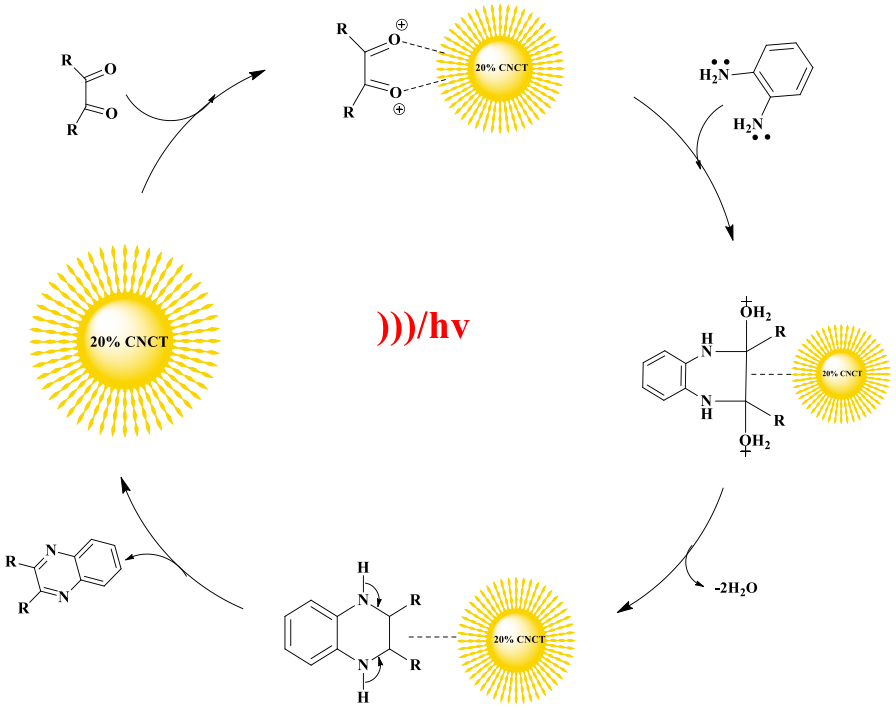

Fig. 7 Possible mechanism in synthesis of Quinoxalines under ultrasonic and visible light irradiation

Table 6 CNCT catalysed synthesis of dihydroquinazolinones under ultrasonication/visible light irradiation[a]

Product	R_1	Time (min)	Yield[b]		Melting point		TON[d]	TOF[d]
			US/vis[c]	Δ[c]	Found	Refs.		
2.3a	H	5	84	19	216–217	[21]	8.2	1.65
2.3b	OCH_3	5	81	23	173–174	[21]	7.9	1.59
2.3c	4-Br	3	98	31	195–195	[23]	9.6	3.21
2.3d	3-Br	3	95	43	183–184	[22]	9.3	3.11
2.3e	4-NO_2	5	82	32	194–195	[21]	8.06	1.61
2.3f	3-NO_2	5	89	29	166–167	[23]	1.75	1.75
2.3h	4-Cl	3	91	27	190–192	[22]	2.98	2.98

[a]Reaction condition: anthranilamide (1 mmol), corresponding aldehyde (1 mmol), catalyst (40 mg) were simultaneously treated with ultrasonic and visible light irradiation

[b]Isolated yields

[c]*US* ultrasonic, *VS* visible light, Δ conventional heat

[d]*TON* turn over number, *TOF* turn over frequency

quinoxaline derivatives. Here, the use of sonication was to refresh the active sites of a g-C_3N_4 surface to produce more cycles. Without sonication also the reaction produces good yields up to ~ 97% in visible light. At that time the reusability of catalyst efficiency also varied (Fig. 8). Mainly sonication activates the catalyst surface and produces more amount of active sites in **1.1**. Cavitations also reduce the activation energy barrier and give the final products **1.3, 2.3**.

Finally, the recovered catalyst from the reaction mixture (Schemes 1, 2) was washed two times with ethanol and one time with water. After washing, the CNCT nanocomposite was dried at 60 °C. This catalyst was used for the same reaction several times without losing its catalytic activity. 20% CNCT shows good activity for the next five cycles as shown in Fig. 8. Compared to the reusability

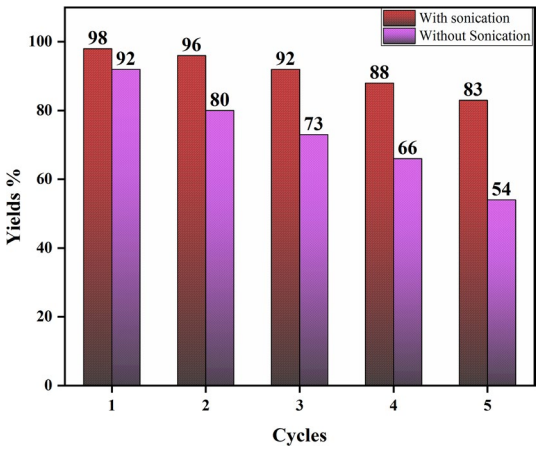

Fig. 8 Reusability of with and without sonication

cycle with and without the sonication test is slightly different, sonication exhibit excellent sonophotocatalytic response.

Conclusion

In conclusion, we have developed a heterogenous g-C_3N_4/Cu_3TiO_4 catalyst as a non-toxic and accessible catalyst. A quick and clean reaction of dihydro-quinazolinone and quinoxaline compounds prepared from benzil, diamines, and aldehydes in ethanol under ultrasound with visible light irradiation was documented. Ultrasonication cleans the active sites in the catalyst surface to enhance the reusability of g-C_3N_4/Cu_3TiO_4. The process is straightforward, begins from readily available commercial starting materials, and provides reasonable yields for biologically interesting goods. The current study demonstrates the benefits of Ultrasound/Visible light assisted heterogeneous catalysis in the synthesis of heterocycles, which are commonly appreciated in a wide range of applications, especially medicinal chemistry and drug development. Furthermore, while heterogeneous catalysis has been known for over a century, recent advances in material science have resulted in a detonation of new functional solid catalysts.

Supplementary Information The online version contains supplementary material available at https://doi.org/10.1007/s11164-021-04461-3.

References

1. S.R. Vemula, D. Kumar, G.R. Cook, Tetrahedron Lett. **59**, 3801 (2018)
2. J.X. Chen, H.Y. Wu, W.K. Su, Chin. Chem. Lett. **18**, 536 (2007)
3. A. Nathubhai, P.J. Wood, M.D. Lloyd, A.S. Thompson, M.D. Threadgil, ACS Med. Chem. Lett. **4**, 1173 (2013)
4. R. Bouley, M. Kumarasiri, Z. Peng, L.H. Otero, W. Song, M.A. Suckow, V.A. Schroeder, W.R. Wolter, E. Lastochkin, N.T. Antunes, H. Pi, S. Vakulenko, J.A. Hermoso, M. Chang, S. Mobashery, J. Am. Chem. Soc. **137**, 1738 (2014)
5. R.Z. Qiao, B.L. Xu, Y.H. Wang, Chin. Chem. Lett. **18**, 656 (2007)
6. H.L. Yale, M. Kalkstein, J. Med. Chem. **10**, 334 (1967)
7. K. Dai, L. Lu, Q. Liu, G. Zhu, X. Wei, J. Bai, L. Xuan, H. Wang, Dalton Trans. **43**, 6295 (2014)
8. S.R. Vemula, D. Kumar, G.R. Cook, ACS Catal. **6**, 5295 (2016)
9. J. Palaniraja, S.M. Roopan, RSC Adv. **5**, 37415 (2015)
10. S.G. Babu, R. Karvembu, Catal. Surv. Asia **17**, 156 (2013)
11. S. Santhisudha, G. Mohan, T.S. Rani, P.V. Reddy, C.S. Reddy, Lett. Drug Des. Discov. **16**, 721 (2019)
12. V.K. Rai, F. Verma, S. Mahata, S.R. Bhardiya, M. Singh, A. Rai, Curr. Org. Chem. **23**, 1284 (2019)
13. F. Akira, K. Honda, Nature **238**, 37 (1972)
14. C. Haojie, W. Xu, Org. Biomol. Chem. **17**, 9977 (2019)
15. T.C. Prathna, N. Chandrasekaran, A.M. Raichur, A. Mukherjee, Colloids Surf. B **82**, 152 (2011)
16. D.D. Priya, M.R. Khan, S.M. Roopan, J. Nanostruct. Chem. **10**, 289 (2020)
17. P. Sharma, Y. Sasson, RSC Adv. **7**, 25589 (2017)
18. R.G. Vaghei, A. Shahriari, Y. Maghbooli, J. Mahmoudi, Res. Chem. Intermed. **43**, 983 (2017)
19. S. Panneri, P. Ganguly, B.N. Nair, A.A.P. Mohamed, K.G.K. Warrier, U. Nair, S. Hareesh, Environ. Sci. Pollut. Res. **24**, 8609 (2017)

20. M. Kumaresan, V. Saravanan, P. Sami, M. Swaminathan, Res. Chem. Intermed. **46**, 4193 (2020)
21. A. Shaabani, A. Maleki, H. Mofakham, Synth. Commun. **38**, 375 (2008)
22. M. Rueping, A.P. Antonchick, E. Sugiono, K. Grenader, Angew. Chem. Int. Ed. **48**, 908 (2009)
23. S.K. Ghosh, R. Nagarajan, RSC Adv. **6**, 27378 (2016)